Deep-Sea Research I 56 (2009) 2100–2114

Contents lists available at ScienceDirect

Deep-Sea Research I

journal homepage: www.elsevier.com/locate/dsri

The Canary Eddy Corridor: A major pathway for long-lived eddies in the subtropical North Atlantic

Pablo Sangrà [a,*], Ananda Pascual [b], Ángel Rodríguez-Santana [a], Francisco Machín [c], Evan Mason [a], James C. McWilliams [d], Josep L. Pelegrí [c], Changming Dong [d], Anna Rubio [e], Javier Arístegui [a], Ángeles Marrero-Díaz [a], Alonso Hernández-Guerra [a], Antonio Martínez-Marrero [a], Maricel Auladell [c]

[a] Facultad de Ciencias del Mar, Universidad de Las Palmas de Gran Canaria, Spain
[b] Instituto Mediterráneo de Estudios Avanzados, IMEDEA(CSIC-UIB), Spain
[c] Departament d'Oceanografía Física, Institut de Ciències del Mar, CSIC, Spain
[d] Institute of Geophysics and Planetary Physics, University of California, Los Angeles, USA
[e] Laboratoire de Physique des Océans, Université de Bretagne Occidentale, France

ARTICLE INFO

Article history:
Received 22 April 2009
Received in revised form
14 August 2009
Accepted 24 August 2009
Available online 11 September 2009

Keywords:
Eddy corridor
Long-lived eddies
Eddies demography
Eddy tracking
Northeastern subtropical Atlantic

ABSTRACT

We report, from remote sensing and *in situ* observations, a new type of permanent structure in the eastern subtropical Atlantic Ocean, that we call the "Canary Eddy Corridor". The phenomenon, is a zonal long-lived (>3 months) mesoscale eddy corridor, whose source is the flow perturbation of the Canary Current and the Trade Winds at the Canary Islands. The latitudinal range of the corridor spans 22°N–29°N and extends from the Canaries to at least 32ºW, near the mid-Atlantic. This is the main region of long-lived westward-propagating eddies in the subtropical northeast Atlantic. From a age-distribution study we observe that at least 10% of mesoscale eddies in this region are long-lived, with a dominance of anticyclones over cyclones. Another four westward-propagating eddy corridors were also detected: two small corridors north and south of the Azores Front; a small zonal corridor located near 31ºN, south of the island of Madeira; and a small corridor located near the Cape Blanc giant filament. The existence of these corridors may change, at least for the northeastern subtropical Atlantic, the general idea that mesoscale eddies are disorganized, ubiquitous structures in the ocean. The Canary Eddy Corridor constitutes a direct zonal pathway that conveys water mass- and biogeochemical properties offshore from the Canary Island/Northwest Africa upwelling system, and may be seen as a recurrent offshore pump of organic matter and carbon to the oligotrophic ocean interior. Estimates of volume and mass transport indicate that Canary Eddy Corridor westward transport is more than one-fourth of the southward transport of the Canary Current. The westward transport of kinetic energy by the eddies of the Canary Corridor is as important as the southward transport by the Canary Current. The total primary production related to the Corridor may be as high as the total primary production of the northwest Africa upwelling system for the same latitude range.

Published by Elsevier Ltd.

1. Introduction

Oceanic structures of order 10–100 km such as fronts and eddies, called mesoscale structures, exert a profound

* Correspondence to: Departamento de Física, Edificio de Ciencias Básicas, Campus Universitario de Tafira, 35002 Las Palmas de Gran Canaria, Spain. Tel.: +34 928454519; fax: +34 928452900.
E-mail address: psangra@dfis.ulpgc.es (P. Sangrà).

0967-0637/$ - see front matter Published by Elsevier Ltd.
doi:10.1016/j.dsr.2009.08.008

influence on the oceanic global circulation, as they may greatly enhance large-scale fluxes of momentum, heat, salt and material tracers (Danabasoglu et al., 2008; Jochum et al., 2008). Additionally, recent observations near ocean fronts and eddies suggest that these structures may produce significant heat fluxes that have a direct impact on the atmosphere (Minobe et al., 2008; Small et al., 2008). Hence, it is important to identify regions of permanent mesoscale structures, as they are likely to exert a profound influence on the ocean–atmosphere system. In the eastern subtropical North Atlantic, three permanent oceanic mesoscale structures have been described: the Azores and Cape Verde frontal regions and the northwest Africa upwelling system. In this study, we report on a new type of permanent structure which comprises a corridor that contains long-lived (life span >3 months) westward-propagating mesoscale eddies generated by the Canary Islands. We call this structure the Canary Eddy Corridor.

Over the last 15 years oceanic eddies generated at the Canary Islands have been intensively investigated (e.g. Sangrà et al., 2007; Arístegui et al., 1994). Cyclones are shed from La Palma, El Hierro, La Gomera and Gran Canaria. Cyclones are also generated close to the African coast south of Fuerteventura (Navarro-Pérez and Barton, 1997). Anticyclones detach mainly from Gran Canaria and Tenerife (Sangrà et al., 2005). The main generation mechanism is the perturbation of the Canary Current by the islands, with the wind shear at the island wake acting as a trigger mechanism that permits eddy shedding at relatively low intensities of the Canary Current (Sangrà et al., 2007; Jiménez et al., 2008). In a recent observational study from 2 years of mooring and remote sensing data, Piedeleu et al. (2009) observed that eddies are more frequently generated in spring and summer with an estimated spin up time of about 10 days.

Most studies have focused on eddies generated at Gran Canaria (Arístegui et al., 1994; Sangrà et al., 2007). During their early stages, the Gran Canaria eddies have radii equivalent to about the island radius, which is close to the internal Rossby deformation radius (25 km), their maximum depth ranges between 300 and 700 m, and the associated isopycnal perturbation is about 40–70 m. At these initial stages the eddies are Rankine-like, rotating in near solid-body rotation (Sangrà et al., 2005, 2007). As they evolve, the radius and rotation period increases (Sangrà et al., 2005, 2007). Cyclones are inertially unstable, and cannot rotate as fast as the more stable anticyclones because of the initial strong anticyclonic shear at their periphery (Sangrà et al., 2007). Anticyclone stability may also be related to strain induced from neighbouring vortices, as cyclonic eddies are more strongly weakened by asymmetric deformation than anticyclones (Graves et al., 2006). Buoy trajectories indicate that both cyclones and, in particular, anticyclones are long-lived eddies, lasting as coherent structures for at least several months (Sangrà et al., 2005, 2007).

Our objective here is to give a first description, from remote sensing and *in situ* observations, of the Canary Eddy Corridor that is built up by oceanic eddies shed by the Canary Islands. We first introduce the methodologies developed to track long-lived eddies from merged altimeter data (Section 2). Next we describe the main characteristics of the corridor and discuss the ability of merged altimeter data to resolve eddies, through comparison of altimeter data with *in situ* observations (Section 3). We then describe, from long-lived eddy trajectories, the five eddy corridors observed in the northeast subtropical Atlantic (Section 4) and discuss the main demographic (age-distribution) characteristics of the Canary Eddy Corridor (Section 5). We finally discuss the importance of the Canary Eddy Corridor upon mesoscale variability and biogeochemical fluxes in the subtropical North Atlantic and present our main conclusions (Section 6).

2. Methodology

2.1. Merged altimeter data

The altimetry data set is based on 14 years (October 1992–September 2006) of gridded absolute dynamic topography (ADT) fields combining several altimeter missions. Previous studies have shown that merging of multiple altimeter missions provides an improved description of mesoscale variability as well as sea-level variations (Pascual et al., 2006, 2007). In particular, this study uses Topex/Poseidon (T/P) data over the 1993–2001 period, Jason-1 (from June 2002), ERS1/2 data (over the 1993 to June 2003 period with a lack of ERS1 data from January 1994 to March 1995) and ENVISAT data (from June 2003). These data are currently delivered by the AVISO web server (Salto/Duacs system, http://www.aviso.oceanobs.com/).

We provide here a summary of the methodology used by AVISO to build the gridded fields (a complete description is available in the SSALTO/DUACS User Handbook, 2006). Briefly, a homogeneous and inter-calibrated sea-surface height (SSH) data set is obtained by performing a global crossover adjustment, using T/P as the reference mission (Le Traon and Ogor, 1998). Then, these data are geophysically corrected (tides, wet and dry troposphere, ionosphere).

The dataset presently provided by AVISO is corrected by a dynamic atmospheric correction based on a combination of the MOG2D barotropic model developed by Legos/CNRS (Carrère and Lyard, 2003) for high frequencies and an inverse barometer correction developed by CLS, assuming a static response of the ocean to atmospheric forcing, and neglecting wind effects for low frequencies. Along-track data are resampled every 7 km using cubic splines, and the sea-level anomalies (SLA) are computed by removing a 7-year mean SSH corresponding to the 1993–1999 period. The mean dynamic topography from Rio and Hernandez (2004) was added to SLA. Measurement noise is reduced by applying Lanczos (cut-off and median filters). The mapping method to produce gridded fields of SLA from along-track data is described in Ducet et al. (2000). The long-wavelength error parameters have been adjusted according to the new geophysical corrections (L. Carrère, pers. comm., 2006). Sea-level anomaly gridded fields are calculated every week on a 1/4° grid.

Absolute dynamic topographic fields are obtained by adding to the SLA fields a mean dynamic topography. Finally, velocities are computed by applying the geostrophic approximation.

2.2. Okubo–Weiss technique for eddy tracking

The Okubo–Weiss parameter (W) has been widely used to detect eddies in the ocean (e.g. Isern-Fontanet et al., 2006). This parameter is defined as

$$W = s_n^2 + s_s^2 - \omega^2$$

$$s_n = \mathrm{d}u/\mathrm{d}x - \mathrm{d}v/\mathrm{d}y$$

$$s_s = \mathrm{d}u/\mathrm{d}y + \mathrm{d}v/\mathrm{d}x$$

where s_n and s_s are the normal and shear components of strain, ω is the relative vorticity and u and v the horizontal components of geostrophic velocity fields as derived from merged altimeter data. Since vortices are regions of concentrated relative vorticity in which there is a dominance of vorticity over strain, we use a threshold value (U_W) for W, so eddies are defined as regions with $W<U_W$. In several studies (e.g. Chelton et al., 2007) the threshold used is $U_W=-2\times10^{-12}\,\mathrm{s}^{-2}$, although in our case the chosen value will be slightly different (see comments about our threshold value below). For eddy tracking, we allocate each eddy to a single point calculated as the centroid from the values at its contour (Chelton et al., 2007); hence, the eddy tracking is actually performed as a centroid tracking. We set closed values of W using U_W values. The centroid is the mean values of the W point closed contour. We define the eddy polarity from the vorticity field. The criteria used to join a centroid detected at t to a trajectory at $t-1$ is based on a search radius (d), so a centroid at t is merged to the closest centroid at $t-1$ with the same polarity if they are separated by a distance lower than the search radius.

Following Isern-Fontanet et al. (2006), we obtain from statistical analysis initial values for U_W, $U_W=-0.2\sigma_W\,\mathrm{s}^{-2}$, which correspond with -1.6×10^{-12} and $-1.7\times10^{-12}\,\mathrm{s}^{-2}$ for zones with positive and negative vorticity, respectively. However, our main interest is the long-lived eddies; although they are detected with relatively low U_W (<$-10\times10^{-12}\,\mathrm{s}^{-2}$), it has been recently documented with *in situ* observations in the Canary Basin that eddies pulsate as they propagate westward (Sangrà et al., 2005), so that U_W could "lose" the eddy, breaking its trajectory and underestimating its actual age. Hence, we test the eddy detection and tracking process using several values for both d (eddy diameter) and U_W, varying d from 30 to 90 km and U_W from -2×10^{-12} to $-14\times10^{-12}\,\mathrm{s}^{-2}$, between June 2004 and February 2005. The trajectory building process monitors step by step for selected intense eddies in the Corridor by comparison with ω and W fields. The best results are obtained with d=40 km and $U_W=-8\times10^{-12}\,\mathrm{s}^{-2}$, which retrieves whole trajectories, avoiding artificial merging with surrounding eddies. For this reason, the threshold used in this work will be $U_W=-8\times10^{-12}\,\mathrm{s}^{-2}$. Using statistical analysis of ω versus W in the study region, we have obtained for $U_W=-8\times10^{-12}\,\mathrm{s}^{-2}$ an absolute value for relative vorticity, $\omega=3.1\times10^{-6}\pm3.4\times10^{-7}\,\mathrm{s}^{-1}$, which is used as a relative vorticity cut-off in the wavelet method (see below).

2.3. Wavelet technique for eddy tracking

We use a wavelet-based utility program for identification of mesoscale eddies in the surface geostrophy velocity fields obtained from satellite sea-level data. The wavelet analysis allows 2D decomposition of a signal into wave packets that have a known position in space which allow the geographic localization of coherent eddy-like structures. For more details on the algorithm used here, the reader is referred to Doglioli et al. (2007). Siegel and Weiss (1997) give a more extensive discussion on the pertinence and details of the wavelet transform. The wavelet technique can work on maps of either SSH anomalies, potential vorticity or Okubo–Weiss criterion, but processing relative vorticity gives good results in terms of eddy identification (Doglioli et al., 2007).

It is worth noting that the results of the wavelet analysis are dependent on some other predefined parameters: (i) the number of spectral coefficients kept for signal reconstruction (only the wavelets with the largest coefficients are kept), (ii) a cut-off criterion applied to the vorticity fields before the wavelet decomposition and, (iii) a cut-off criterion based on eddy size applied to the identified structures (Doglioli et al., 2007). As noted by Doglioli et al. (2007) the percentage of spectral coefficients kept for signal reconstruction is a critical parameter of the analysis. In this case the best results are obtained with percentages between 8% and 11% (higher percentages increase noise in pattern recognition and lower percentages involve losing part of the mesoscale signal).

The results of the analysis are also sensible to the cut-off criteria mentioned above; for this reason, and to make a fair comparison of both methods, the cut-off values have been chosen in order to be equivalent to the ones used with the Okubo–Weiss technique. As already mentioned, to find the correspondence between the relative vorticity and Okubo–Weiss cut-off criterion, we have analyzed statistically the mean values of relative vorticity of eddies detected through the whole period (1992–2004) by the Okubo–Weiss technique using a cut-off value of $W=-8\times10^{-12}\,\mathrm{s}^{-2}$. The corresponding cut-off vorticity absolute value for relative vorticity is around $\omega=3.1\times10^{-6}\pm3.4\times10^{-7}\,\mathrm{s}^{-1}$. After some tests, the vorticity cut-off criteria has been set to a lower value ($\omega=2\times10^{-6}$) to compensate for the part of the signal lost with the smallest spectral coefficients that are disregarded when the wavelet reconstruction is done. Finally, as the Okubo–Weiss technique used here is not able to discriminate between eddy sizes, no restrictions have been imposed in terms of eddy size in the wavelet analysis. After extracting coherent eddy patterns from the successive relative vorticity fields, the center of an eddy is determined by the maximum value of this variable. The criterion used to compute trajectories is based, as in the previous case, on a search radius (d). In this case we use a search radius of r=60 km.

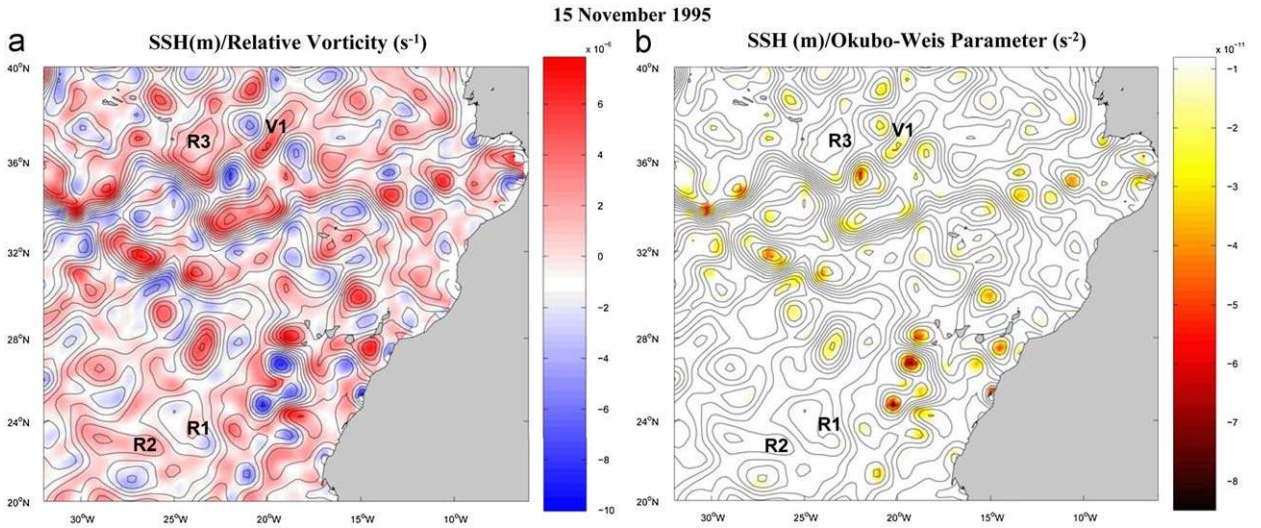

Fig. 1. Distribution of (a) contours of sea-surface height (SSH) superposed on the relative vorticity field (colours) in the northeastern subtropical Atlantic as obtained from merged altimeter data for 15 November 1995. (b) Corresponding contours of SSH superposed on the relative Okubo–Weiss field (colours) for those values of the Okubo–Weiss parameter larger than $W=-8\times10^{-12}\,s^{-2}$. This value was chosen as the W threshold to detect eddies (see Section 2.2).

2.4. Comments on flow visualization

Both Okubo–Weiss and wavelet techniques are based on detecting eddies as centroids of relative vorticity around a maximum vorticity value. For a non-stationary flow, streamlines, trajectories and streak-lines usually do not coincide. These differences are very large for barotropic flows passing obstacles (e.g., Eaton, 1987). In our study we associate eddies with vortices, which in the barotropic case coincide with streak-lines but not with streamlines (as obtained from SSH, Jiménez et al., 2008). Although SSH matches well with vortices south of the Canaries, there is some mismatch at the frontogenesis regions of the Azores Front located at 34°N (Fig. 1). If an unstable region does not maintain coherence that would lead to vortices (e.g. vortex V1 in Fig. 1b), it is rapidly filtered out by our methodologies. Notice also that SSH closed structures associated with large meanders of the front have their maximum vorticity at their periphery (see elongated structure south of V1 in Fig. 1b). These structures may be the signal of eddies related to westward-propagating Rossby waves that are also filtered out by our methodology. Notice also that many large closed SSH structures, that do not have a clear maxima at their center in the vorticity field, are also filtered out (see eddies R1–R3 in Fig. 1b).

3. Description of the Canary Eddy Corridor

The existence of the Canary Eddy Corridor was suggested to us by previous isolated observations of *Swesties* (shallow subtropical subducting westward-propagating eddies, Pingree, 1996). Swesties are anticyclonic, long-lived eddies (a few years life span) that originate south of the Canary Archipelago. Swesty sea-level anomalies have been observed as far west as 50°W, well beyond the mid-Atlantic Ridge (Pingree and Garcia-Soto, 2004). The main properties of Swesty sea-level anomalies were westward propagation with decay of 1° longitude per month or ~12° in a year, with ~50% decay of central SSH. As seen in the Supplementary Movie, the anticyclone trajectory started at 27°N–19°W on 14/10/92 and ended at 25°N–24°W on 28/04/93; this could be the origin of Swesty as observed by Pingree (1996).

The Canary Eddy Corridor is a recurrent feature in 14 years of merged altimeter data, and is a permanent structure in the northeastern subtropical Atlantic (Fig. 2). Because of the strong variability induced by eddy generation and interaction south of La Gomera, Tenerife and Gran Canaria (Sangrà et al., 2005), the precise island origin cannot always be well established from merged altimeter data. Further, the interpolation of altimeter data fails in the vicinity of land, and also the initial size of the eddies is close to the Rossby deformation radius (25 km), below the resolution (diameter) of the merged altimeter data (100 km). To visualize westward propagation of eddies along the corridor is also sometimes rather difficult because of both eddy merging/splitting and their intermittent pulsations in shape and intensity (see Supplementary Movie). Eddy pulsations along their lifetimes have already been observed in the buoy orbits of an intense anticyclone (Sangrà et al., 2005). These pulsations may have been related to eddy/wind interaction that can alter their secondary circulation (Martin and Richards, 2001).

In the 1992 altimeter image, three cyclones (21°W, 24°W and 27°W) and one anticyclone (20°W) propagate westward and exit the domain at 27°N, forming a narrow corridor (Fig. 2a). In the 1997 image, the eddies track westward through a broader corridor that extends from 24°N to 29°N (Fig. 2b). The northern portion of the corridor includes two cyclones (24°W and 20°W) and one anticyclone (22°W). This anticyclone is not generated by

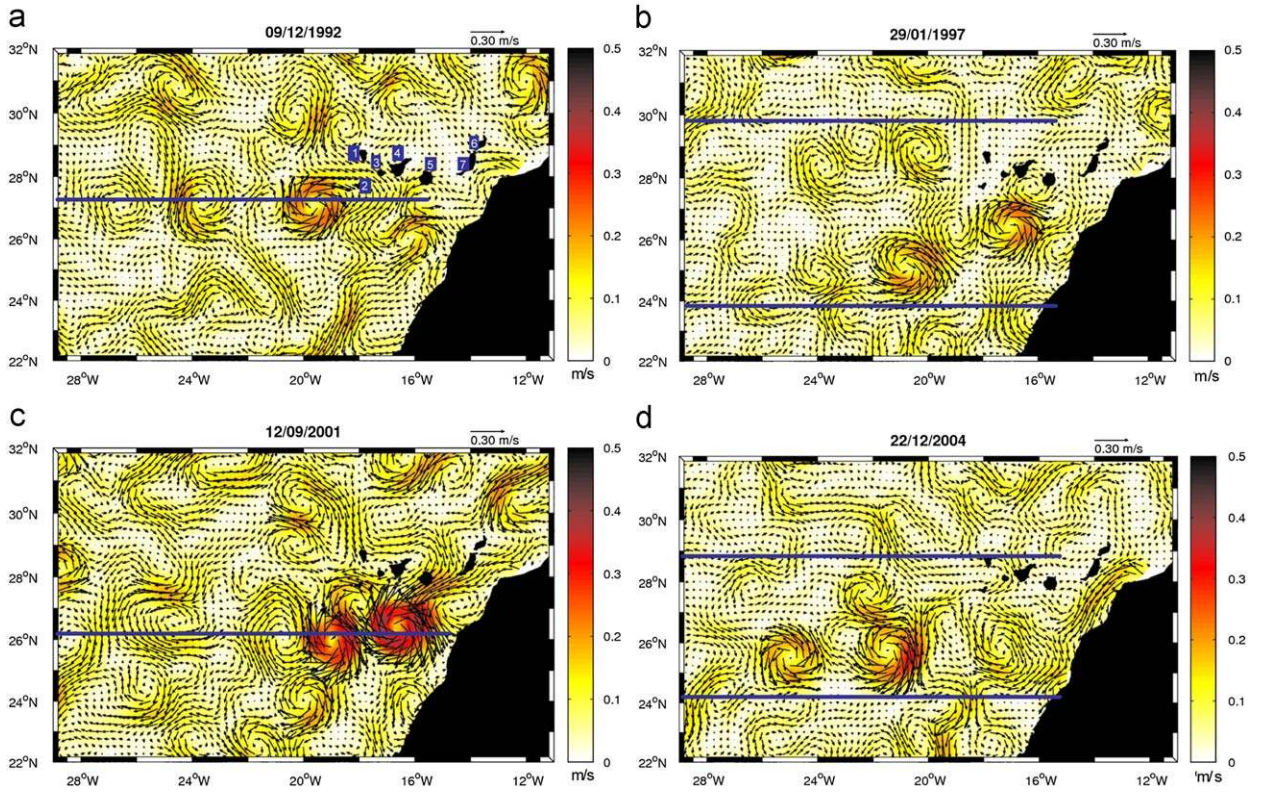

Fig. 2. Selected images of geostrophic velocity fields as derived from merged altimeter data, showing the Canary Eddy Corridor. Blue bold lines indicate either the axis of the corridor (a, c) or its latitudinal extension (b, d). Islands are identified in panel (a) as: 1—La Palma, 2—El Hierro, 3—La Gomera, 4—Tenerife, 5—Gran Canaria, 6—Lanzarote and 7—Fuerteventura.

the Canary Islands, as it entered the corridor from north of La Palma in September 1996. In the 2001 image two intense anticyclones (17°W and 19°W) and three cyclones (18°W, 21°W and 26°W) propagate and exit west at 27°N within a relatively narrow corridor (Fig. 2c). In this instance it was possible to follow the two anticyclones from birth at the islands. The eastern anticyclone was generated at Gran Canaria in August 2001 and left the domain 1 year later at 25°N. The western anticyclone was generated at Tenerife in July 2001 and exited the domain 1 year later at 24°N. The eastern cyclone was observed south of El Hierro in September 2001 and was no longer detected 4 months later when it reached 21°W. The middle/western cyclones were first observed south of El Hierro in March/May 2001, and departed from the domain 9 months later at 26°N/27°N. In the 2004 image a broad zonal corridor was again observed to extend between 24°N and 29°N. This corridor was formed by two cyclones that exited at 28°N, and by two anticyclones and two cyclones that departed at 26°N.

In order to test the robustness of the altimeter-derived data we compare it with other data sources such as drifter trajectories (Figs. 3a, b, and d), acoustic Doppler current profiler (ADCP) data (Fig. 3c) and chlorophyll SeaWIFS images (Fig. 4). ADCP data were collected during the COCA II cruise (May–June 2003), when the drifter of Fig. 3d was also launched. All three drifter trajectories were calculated by interpolating the raw Argos data every 3 h and using a low-pass filter in order to remove inertial oscillations: ~26.5 h). The drifter drogues were set at 100 m in order to avoid wind contamination.

On 29 June 1998 we deployed three drifters into an intense anticyclone (hereafter identified as J98), shortly after its formation south of Gran Canaria (Sangrà et al., 2005). Buoy trajectories clearly match the altimeter observations of this eddy in September (Fig. 3a) and December (Fig. 3b) 1998. The eddy radius, as derived from the drifter trajectories, increased from ca. 25 km in June to ca. 40 km in September. The eddy intensity, as inferred from the buoy periods, decreased from an initial rotating period of 3 days in June to 6 days in September. J98 was not observed in the altimeter data until September because of the limited altimeter resolution (100 km), its interaction with other eddies (Sangrà et al., 2005), and limitations in the altimeter interpolation scheme near land. The last few months of the track of this eddy match that of the Swesty observed by Pingree and Garcia-Soto (2004). The intense western companion eddy originated at Tenerife, as observed in SST images (Sangrà et al., 2005).

Eddy J98 first propagated south until it reached 26°N in September and then moved westward. Eddy propagation depends on the relative importance of the background-flow intensity and the latitudinal change in the local planetary rotation rate (β-effect) across the eddy, which increases with eddy diameter (Willett et al., 2006; Cushman-Roisin et al., 1990). Our altimeter observations

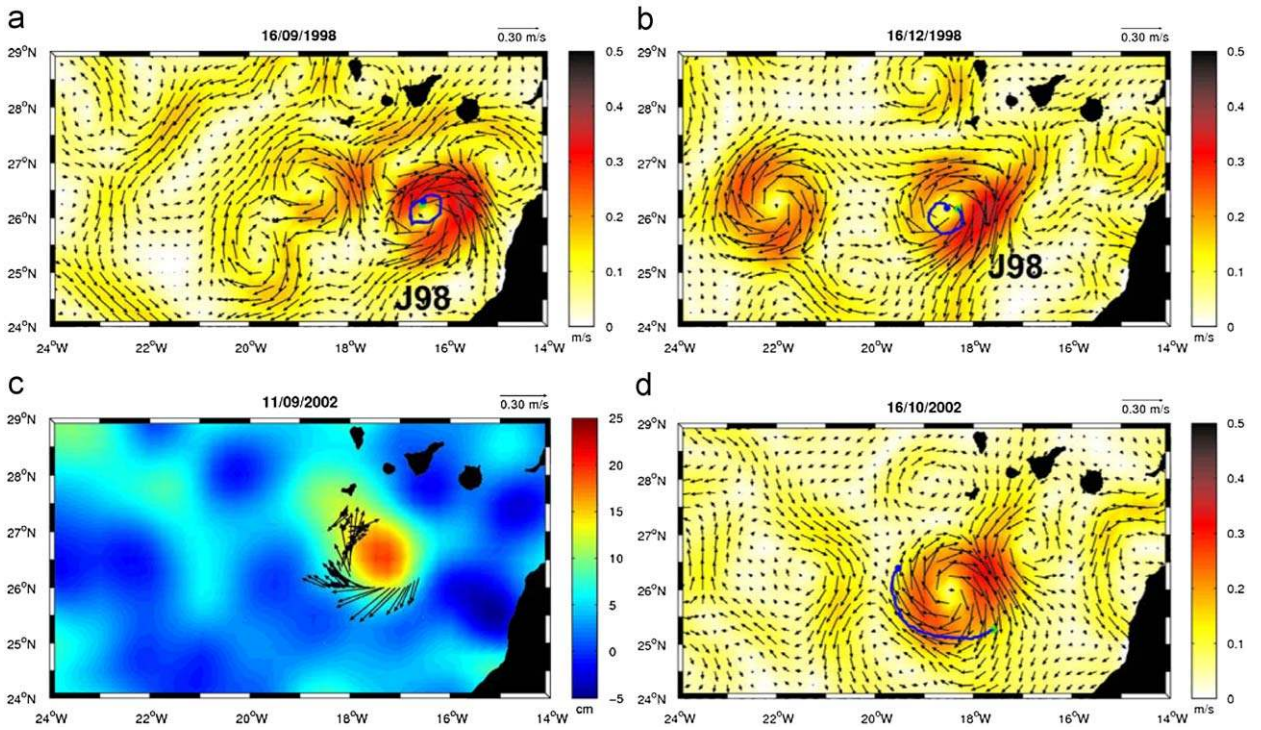

Fig. 3. Comparison of merged altimeter data with other data sources: (a) and (b) a sequence of two images (3 months apart) showing geostrophic velocities superposed onto a drifter trajectory indicated by a blue line. The trajectory corresponds to 3 days before and after the corresponding image, tracking the center of an intense anticyclonic eddy south of Gran Canaria (eddy J98). (c) Black arrows indicate depth-averaged (0–100 m) velocities as obtained from ADCP data, superposed onto sea-surface height as derived from merged altimeter data. Both data sources show an intense anticyclonic eddy south of El Hierro. (d) Geostrophic velocities superposed onto a drifter trajectory indicated by a blue line. The trajectory corresponds to 15 days before and after the corresponding image, tracking the periphery of the same anticyclonic eddy observed in (c), but now 1 month later.

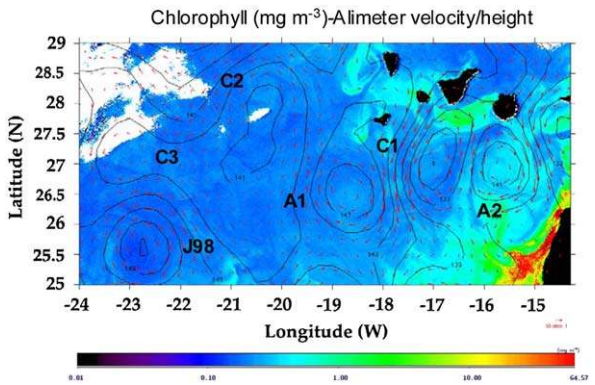

Fig. 4. Chlorophyll concentration (24/04/99) superposed onto sea-surface height and geostrophic velocity as obtained from merged altimeter data (28/04/1999), showing that altimeters may resolve mesoscale eddies far away from the Canary Archipelago but fail close to the islands.

and drifter trajectories indicate that westward propagation dominates except during the initial stages, when the eddies are relatively small and located in the path of the southward Canary Current. We may talk of an inflection point when the westward velocity component exceeds the southward component. This point occurs at about 18ºW, 25ºN, when older eddies have drifted out of the path of the Canary Current and get large enough for the β-effect to become dominant. On average, eddies propagate westward at about 1° per month. As an example, eddy J98 was observed in September 1998 at 17°W and 7 months later at 23°N, having become much less intense (Fig. 4). This eddy left the domain in October 1999, 16 months after its generation. The Tenerife anticyclone leaves the domain in July 1999.

In the September 2002 image we again examine an intense anticyclonic eddy, its altimeter-derived velocities also in good agreement with the ADCP data (Fig. 3c) and the drifter trajectories (Fig. 3d). This eddy detached from Tenerife in August 2002 and left the domain 1 year later at 24°W. The joint data set shows the anticyclonic eddy to be well-resolved in both sea-surface altimetry and ADCP velocity data. The shape and eddy intensity from both data sources coincide well. If we set the eddy periphery to be the region of maximum intensity of the tangential velocity, the eddy size from both data sources is indeed close to 100 km (Fig. 3d).

The chlorophyll images and the altimeter sea-surface height also display good agreement, such as for eddies J98, A1, C1 and A2 (Fig. 4), except close to the islands. As an example, cyclones attached to La Palma and Gran Canaria are not seen in the altimeter data. The cyclones (C2 and C3) west of La Palma are barely resolved by the altimeter data. In contrast, the cyclone (C1) and anticyclone (A2) spawned at Gran Canaria are observed in the image, but appear more distorted in the velocity altimeter data.

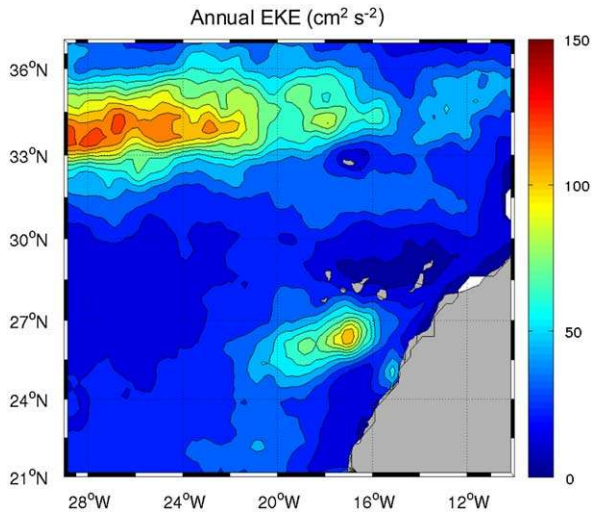

Fig. 5. Annual-mean eddy kinetic energy (EKE) showing the main sources of EKE in the northeastern subtropical Atlantic: the Azores Front and the Canary Archipelago.

Anticyclone A1, generated at Tenerife in February 1999, merged with another anticyclone and left the domain 1 year later at 24°W. Cyclone C1 exited the domain 14 months later at 30°N. Anticyclone A2 strongly interacts with other eddies before leaving the domain.

From the weekly SSH we may calculate the annual-mean field, which provides the large-scale geostrophic velocities, and the weekly anomalies are calculated as the difference. From these anomalies we may hence compute the mean annual eddy kinetic energy (EKE) distribution in the eastern subtropical North Atlantic (Fig. 5). This shows that the main sources of EKE are the Azores front and south of the Canary Archipelago (Fig. 5). These observations match rather well with those of Fig. 9 of Pingree and Garcia-Soto (2004). The tongue of large EKE values associated with the Canary Islands is observed to be initiated about 100 km south of the islands, at 26.5°N, because of the inability of the altimeter to track small eddies close to the islands, and stretches southwest along the eddy corridor, centered at 25°N. The seasonal variability of the EKE shown has highest values south of the archipelago in spring, summer and autumn. Except for autumn, this coincides with the main periods of eddy generation by Gran Canaria observed from in situ data by Piedeleu et al. (2009). The autumn mismatch is due to the fact that eddies take at least 2 months to grow sufficiently so that they are resolved in merged-satellite data, as is the case for anticyclone J98.

4. Eddy corridors in the northeastern subtropical Atlantic

To reveal the signal of westward-propagating eddy corridors in the northeastern subtropical Atlantic we have used merged altimeter data to compute westward-propagating eddy trajectories and demography (Figs. 6 and 7). We use two different techniques, one based on the Okubo–Weiss parameter and the other based on a wavelet analysis (see methodology section). The similar results obtained from both methodologies highlight the robustness of the analyses. In both cases, long-lived westward eddy trajectories reveal four structures in this region (Figs. 6a and 7a): two small corridors north and south of the Azores Front; a small zonal corridor located near 31°N, south of the island of Madeira; the Canary Eddy Corridor; and another small corridor located near the Cape Blanc giant filament, which is a region of intense along-slope flow convergence (20–22°N; Pelegrí et al., 2006; Gabric et al., 1993). The Canary Eddy Corridor extends from 22°N to 29°N and is populated mainly by anticyclones generated south of Tenerife and Gran Canaria.

The dominance of anticyclones over cyclones in the Canary Eddy Corridor is related to their longer life expectancy. Eddy life expectancy depends both on initial intensity and interaction with other eddies (see Supplementary Movie). More stable anticyclones may initially rotate two times faster than cyclones (Sangrà et al., 2007). As shown in Figs. 6a and 7a, as eddies progress west, anticyclones have a tendency to be deflected south whereas cyclones shift north, a characteristic also observed in other regions (Chelton et al., 2007). The southward deflection of anticyclones leads sometimes to merging with eddies generated near the Cape Blanc giant filament, related to the Cape Verde frontal zone. Our methodology considers only those tracks that start 3 months before reaching the western boundary; hence those long-lived eddies that are generated inside the domain but exceed the age of 3 months beyond the boundaries of the domain are not considered.

5. Canary Eddy Corridor demographics

Although a high percentage of the eddy population breaks down, feeding the submesoscale/mesoscale background eddy turbulence, a significant fraction (ca. 10%) is composed of long-lived (life span >3 months), coherent structures (Figs. 6b and 7b). The Okubo–Weiss technique shows 237 long-lived eddies within the 14-year altimeter dataset, giving an average of 17 eddies per year (Fig. 6c). As illustrated in Figs. 6c and 7c, the age pyramid for long-lived eddies (with age defined as the duration of their trajectories) shows a significant skew towards an increase in the anticyclone/cyclone ratio with eddy age, confirming the longer life expectancy for the more stable anticyclones.

In Fig. 8 we showed eddy trajectories lasting between 3 and 6 months, as obtained with the Okubo–Weiss technique from 14 years (1992–2006) of merged altimeter data. The eddy trajectories become fragmented mainly west of 23°W, when eddies are about 6 months old. In these cases many more eddies leave the domain between 22°N and 24°N than for the case of trajectories greater than 6 months. The number of eddy trajectories that last longer than 6 months within the Canary Corridor is underestimated, whereas the number of trajectories that last between 3 and 6 months is overestimated. This is partly related to the eddies' pulsations which produce an

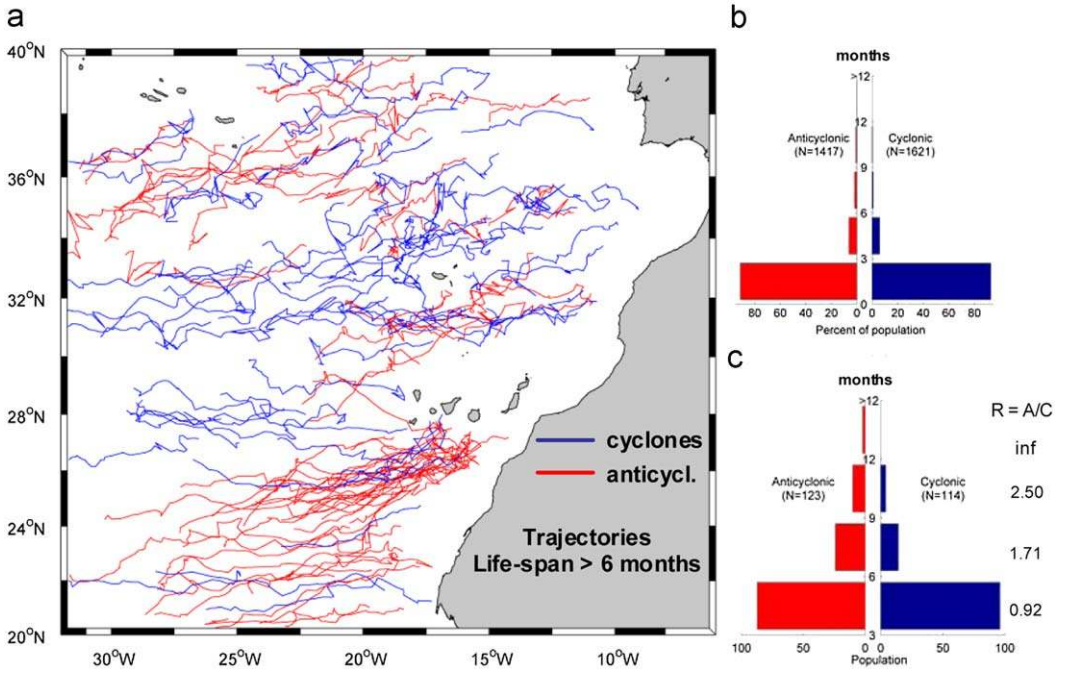

Fig. 6. (a) Westward-propagating eddy trajectories lasting over 6 months, as obtained with the Okubo–Weiss technique (Okubo–Weiss parameter=$-8\times10^{-12}\,s^{-2}$, search radius=40 km) from 14 years (1992–2006) of merged altimeter data, showing the Canary Eddy Corridor extending from 22°N to 29°N. Eastward propagating eddies and near-stationary eddies (westward propagation of less than three degrees) were filtered out. This affects only the eddy field of the Azores front that was depressed, (b) age pyramid for all eddies in the Canary Eddy Corridor region, and (c) age pyramid for long-lived eddies (life span >3 months) in the Canary Eddy Corridor region. The ratio *R* between the number of anticyclones and cyclones increases with eddy age.

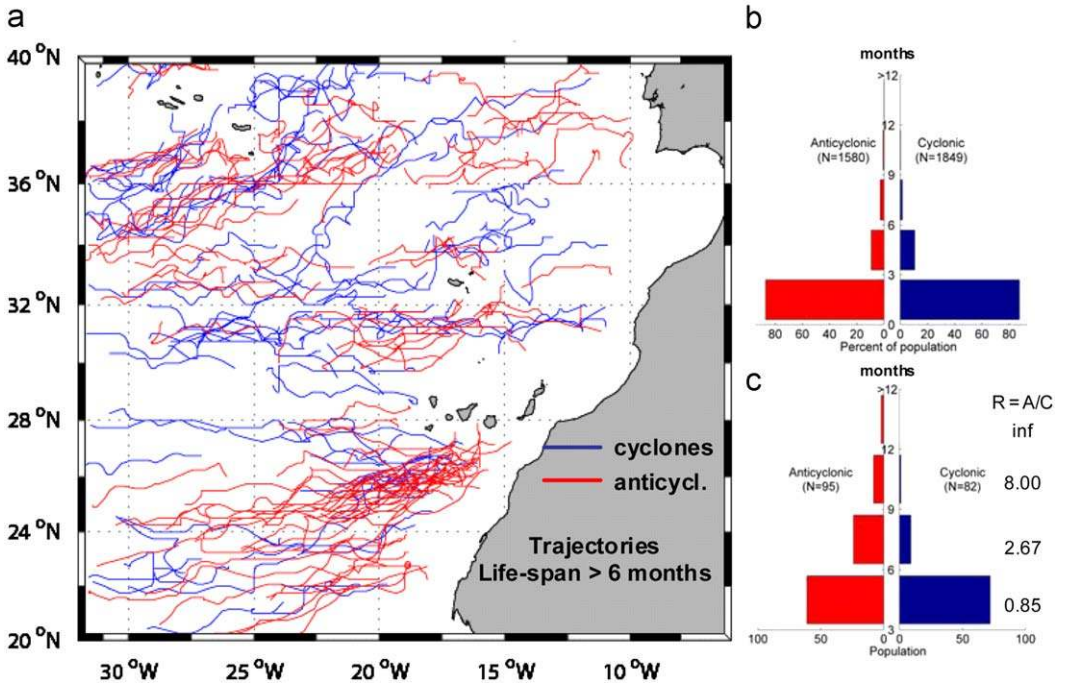

Fig. 7. (a) Same as Fig. 6 but now using the wavelet technique (search radius=60 km). Notice the good qualitative agreement with the results from the Okubo–Weiss technique (Fig. 6).

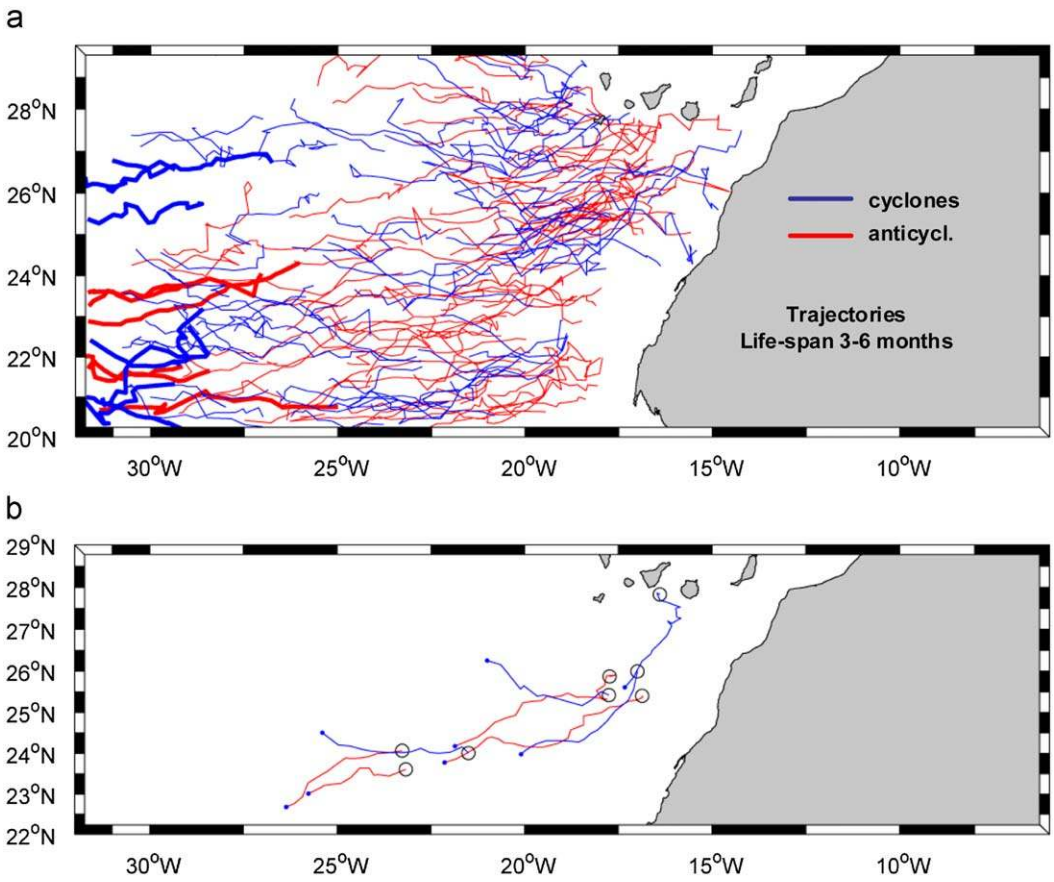

Fig. 8. (a) Eddy trajectories lasting between 3 and 6 months, as obtained with the Okubo–Weiss technique (Okubo–Weiss parameter=$-8\times10^{-12}\,s^{-2}$, search radius=40 km) from 14 years (1992–2006) of merged altimeter data. The eddy trajectories become fragmented mainly west of 23°W, when eddies are about 6 months old. In these cases many more eddies leave the domain between 22°N and 24°N than for the case of trajectories greater than 6 months (Fig. 6a); final segments are indicated by bold lines. Mean length of segments is 3.2 ± 1.1°W for anticyclones and 2.9 ± 0.7°W for cyclones. (b) Selected segmented trajectories showing that they end and restart far from the source region (Canary Islands), suggesting that trajectories for eddies with ages greater than 6 months are underestimated, whereas trajectories for eddies lasting between 3 and 6 months are overestimated. Circles indicate the start locations of the trajectories and dots the end locations.

intermittent decrease/increase of their intensity and shape (Sangrà et al., 2005), in some instances causing the altimeter to miss the eddy so that some trajectories appear as if they end and restart far away from the eddy source region south of the Canary Archipelago (Fig. 8). Fragmented trajectories may also result because of the temporally and spatially changing merged-satellite resolution (D. Chelton, personal communication). An additional cause of tracking loss may be anticyclonic eddy subduction (Pingree, 1996). Consecutive 3- and 4-month fragmented eddy trajectories do suggest that many eddies near the mid-Atlantic (32°W) 4 months after their generation, mainly between 22°N and 24°N (Fig. 7a).

As indicated in Table 1 and illustrated in Fig. 9, the main parameters of the five corridors show that the Canary Eddy Corridor is the main region of eddies with life-span greater than 6 months, accounting for the 42% of long-lived eddies in the northeastern subtropical Atlantic. We select long-lived eddies to be 6 months or older because of fragmented trajectories of younger eddies as pointed out above (see Fig. 8). As seen in Fig. 9, eddies that originated to the south and north of the Azores Front corridors do not have a well-defined source region, extending zonally all along the front. However, the Madeira corridor and Canary Eddy Corridor have well-defined source regions. Some eddies of the South Azores Front Corridor correspond to storms that are cyclonic eddies propagating westward around 32.2°N, observed from in situ data by Pingree and Sinha (2001). Other storm eddies of this corridor were tracked by Pingree et al. (1999), from remote sensing and *in situ* data. Therefore, we think that an adequate name for this corridor would be the Storm Corridor. The Madeira corridor has two source regions, the island of Madeira and the Cape Ghir filament region, close to the African coast at 32°N. Eddies shedding from the Cape Ghir filament were previously reported from *in situ* and SST images (Pelegrí et al., 2005a, b). The eddy source of the Canary Eddy Corridor is clearly the Canary Islands (Table 2). Notice that some eddies originate far away from the archipelago. As already pointed out, this is related to the fragmentation of eddy trajectories.

Table 1
Main corridor parameters showing that the Canary Eddy Corridor is the main region of long-lived eddies, accounting for the 42% of long-lived eddies, in the northeast subtropical Atlantic.

Corridors	Life span >6 month		
	Latitude propagating range	No. of eddies	Fraction (%)
North Azores Front	35–38°N	26	22
South Azores Front	33–35°N	19	16
Madeira	31–33°N	20	17
Canary	**22–29°N**	**50**	**42**
Cape Blanc	20–22°N	4	3

The second through fourth columns show information on the propagation of long-lived eddies along five eddy corridors: latitude ranges, number of propagating eddies, and percentage of total population.

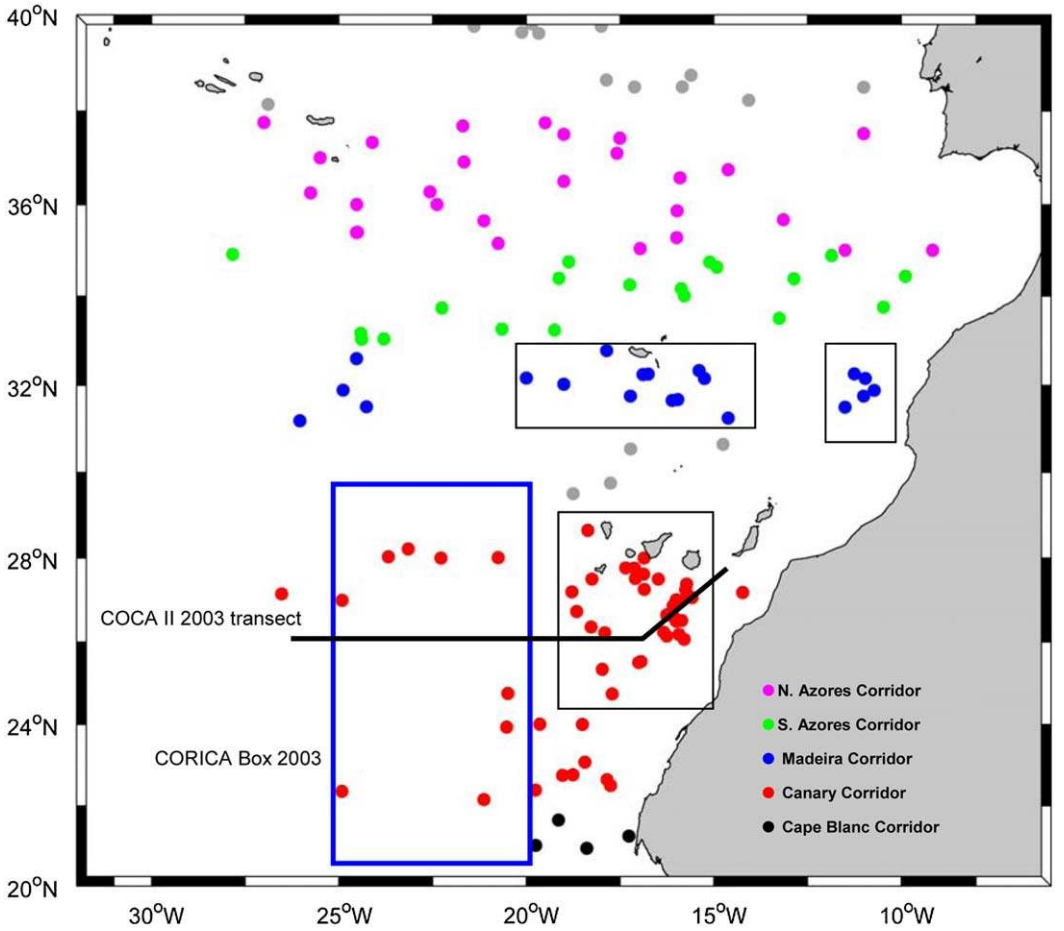

Fig. 9. Location of origin for eddies lasting more than 6 months in the northeastern subtropical Atlantic. Main source regions are identified by a black frame. Notice that the Canary Islands are the main source for these eddies. The Azores corridors do not have a well-defined source region as they originate all along the front.

6. Discussion and conclusions

This study gives a first description of the Canary Eddy Corridor, a zonal, long-lived eddy corridor in the northeastern subtropical Atlantic. This corridor is the principal region of westward-propagating long-lived eddies in the northeastern subtropical Atlantic. Its westward extension, for 1-year-old trajectories, reaches at least as far as 30°W, probably more if we were to consider more diffuse eddies.

The study also shows that merged altimeter data and eddy tracking techniques are valuable tools to describe eddy demographics in oceanic regions where eddy radii

Table 2
Comparison of the Canary Eddy Corridor and Canary Current (see Section 6).

	Transp. volume TrV (Sv)=$TAh\times10^{-6}$	Transp. mass TrM (kg s^{-1})=$TrV\rho\times10^{6}$	Kinet. ener. transp.un. mass KET (m^2 kg s^{-3})=$EKE\rho TA$
Canary Eddy Corridor ρ (1027 kg m^{-3})	1.3	1.3×10^{9} (0.7×10^{9})[a]	43,481
	Transp. volume TcV (Sv)=$vLh\times10^{-6}$	Transp. mass TcM (kg s^{-1})=$TcV\rho\times10^{6}$	Kinet. ener. transp.un. mass KCT (m^2 kg s^{-3})=$L\rho v^3$
Canary Current Mean v=0.05 m s^{-1} Mean width, L=300×10^{3} m	4.5 (4.5[b])	4.6215×10^{9}	38,513
Ratios	TrV/TcV=29%	TrV/TcV=28%	KET/KCT=100%

TA (m^2 s^{-1}) is the transported area by the total number of eddies (17 per year); this area was calculated by multiplying the mean eddy radius (r=50 km), depth (300 m) and area (πr^2) by the number of eddies per year. EKE (0.01 m^2 s^{-2}) is the eddy kinetic energy of a single eddy.
[a] Estimate of net westward transport from surface to 300 m, in the CORICA box (see Fig. 9) from Alonso-González et al. (2009).
[b] Estimate of southward volume transport from the surface to 300 m and between 16°N and 19°N, from Hernández-Guerra et al. (2005).

Table 3
Comparison of primary production in the Canary Eddy Corridor, Canary Current and Northwest Africa Upwelling System in order to reveal the importance of the corridor (see Section 6).

	Pri. prod. per eddy PE (g C m^{-2} d^{-1})	Mean pri. prod. upwelling PU (g C m^{-2} d^{-1})	Total upw. PP PUT=PU*W*LU[a] g C d^{-1})	Total PP Canary Eddy corridor PET=PE*A (g C d^{-1})
Primary production	1.6, 1.5, 0.6[b]	2.4 ± 1.5	11.6×10^{10}	10.9×10^{10}

[a] W is the mean width of the upwelling, W=60 km, and LU is the Canary Eddy Corridor meridional extension, LU=777 km (22–29°N).
[b] 1.6, Canary Cyclone (Barton et al., 1998); 1.5 Hawaii cyclone (Benitez-Nelson et al., 2007); 0.6 Anticyclone west subtropical North Atlantic (McGillicuddy et al., 2007). We chose a value of 1 g C m^{-2} d^{-1} (see text).

are larger than 50 km. These techniques open up observational approaches to the study of mesoscale eddy dynamics, such as eddy merging/splitting, propagation and stability. The Canary Eddy Corridor is a suitable region for such studies. The existence of this corridor could change, at least for the northeastern subtropical Atlantic, the general idea that mesoscale eddies are disorganized ubiquitous structures in the ocean. It is likely that zonal, long-lived eddy corridors are present in other oceanic regions that have an important source of eddy kinetic energy, such as in the lee of the Hawaiian Islands (Calil et al., 2008).

6.1. Impact on mesoscale variability

As clearly illustrated in Fig. 9, the Canary Islands are the main source region of long-lived eddies in the northeastern subtropical Atlantic. This is also supported by the distribution of EKE, which shows a maximum of eddy activity south of the Canaries (Fig. 5). This corridor provides a striking contrast with the southward-directed background flow (Canary Current). It conveys mesoscale turbulence along a latitudinal band and serves as a westward conduit that transports properties from the relatively cold eastern ocean boundary and the northwest Africa upwelling system.

In order to get a first approach of the importance of the Canary Eddy Corridor on westward transport of volume, mass and kinetic energy, we have computed these parameters and compared them with available estimates of the southward-flowing Canary Current (Table 3). Westward volume and mass transport by the 17 eddies generated yearly in the Canary Eddy Corridor are TrV=1.3 Sv and TrM=1.3×10^{9} kg s^{-1}, respectively. For these calculations we have chosen a mean eddy radius of r=50 km (see Fig. 4) and a mean eddy depth of 300 m (Arístegui et al., 1994; Sangrà et al., 2005, 2007). As eddies are Rankine-like (near cylindrical) we have assumed a cylindrical shape for area and volume calculations. The Canary Eddy Corridor volume and mass transports contribute approximately one-fourth of the southward transport by the Canary Current (4.5 Sv, see Table 3). Mass transport is relatively close to the net westward transport observed by Alonso-González et al. (2009) in the CORICA CTD box (Fig. 9). This box was located westward of the Canaries, outside the Canary Current axis, where the transport is mainly zonal. The above estimates suggest that eddies in the Canary Eddy Corridor are the main source of westward transport of properties in the northeastern subtropical Atlantic; this transport is significant when compared with the southward transport by the Canary Current.

To estimate the EKE transport by the Canary Eddy Corridor we have chosen a mean annual value of 0.01 m^2 s^{-2} (Fig. 5). In Fig. 10 we show an image of the EKE corresponding to the eddies of Fig. 2a. Values range between 0.025 m^2 s^{-2} for intense eddies and 0.01 m^2 s^{-2}

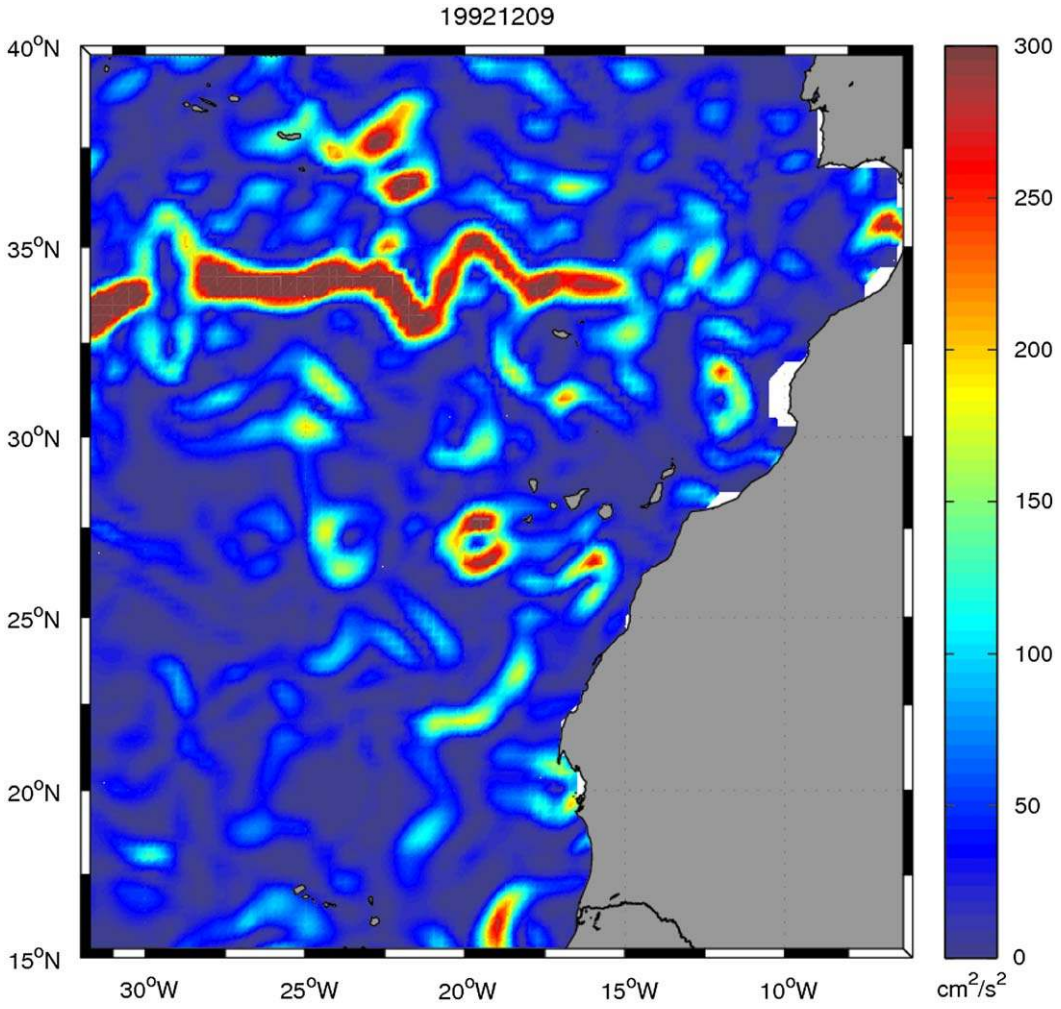

Fig. 10. Eddy kinetic energy (EKE) for 9 December 1992. Notice the clear signal of eddies illustrated in Fig. 2a.

for low-intensity eddies. However, when the annual-mean EKE is calculated, we only observe high values at the source region, south of the Canaries, due to eddy propagation and associated energy scattering (Fig. 5). In order to compare EKE with kinetic energy related to the Canary Current southward flow we estimated, from the COCA II north transect (Fig. 9), a mean velocity of v=0.05 m s^{-1} and a mean width of L=300 km for the Canary Current. These values are in agreement with those reported by Navarro-Pérez and Barton (2001) and by Hernández-Guerra et al. (2005). As shown in Table 3, the westward transport of kinetic energy by eddies of the Canary Eddy Corridor is as important as the southward transport by the Canary Current. Mesoscale eddies are not well resolved in climate models and instead are parameterized as a viscous term playing an important role in energy and momentum dissipation (Jochum et al., 2008). A global eddy demography needs to be established, as already started by Chelton et al. (2007), in order to properly parameterize the global importance of mesoscale long-lived eddies, both as a local energy modulation mechanism and in the large-scale transport of properties.

6.2. *Impact on modulating biogeochemical fluxes*

There is growing evidence that mesoscale eddies modulate biological production and related biogeochemical fluxes (Lévy, 2008; Benitez-Nelson et al., 2007; McGillicuddy et al., 2007). Thus, the Canary Eddy Corridor may be significant not only as a zonal conduit carrying properties from the upwelling region, but also as a modulating factor on the marine system and related biogeochemical fluxes in the northeastern subtropical Atlantic. Primary production (PP) inside eddies is mainly modulated by secondary circulation. Upward Ekman pumping in cold-core cyclonic eddies will lead to an increase of PP through nutrient injection to the euphotic zone, whereas downward Ekman pumping in warm-core anticyclones will lead to a deepening of the mixed layer and a depletion of nutrients, decreasing PP.

The secondary circulation inside an eddy may, however, vary during its life span, leading to eddy pulsation. For eddy J98, we observed convergence/divergence that modified the eddy diameter and intensity during its life span (Sangrà et al., 2005). This eddy was tracked by drifters for seventh months. Eddy pulsations were also observed on cyclones shed by the island of Gran Canaria (Sangrà et al., 2007). Martin and Richards (2001) associated time-varying Ekman pumping velocity with wind pulses. Wind-stress curl causes upward and downward Ekman pumping velocities in anticyclones and cyclones, respectively. McGillicuddy et al. (2007) related wind pulses with extraordinary plankton blooms inside anticyclones. This concept changes the classical view that inside cyclonic eddies secondary circulation leads to upward velocities, and inside anticyclones to downward velocities.

As illustrated in Fig. 4, at the western flanks of the Canary Islands there is a clear increase of chlorophyll due to intense shear and upward Ekman pumping velocity at the initial stages of cyclones (Arístegui et al., 1997). As in anticyclone A2, Gran Canaria anticyclones may entrain high-chlorophyll water from their interaction with upwelling filaments (Arístegui et al., 1997; Pacheco and Hernández-Guerra, 1999). Far from the Archipelago there is also a clear enhancement of chlorophyll by eddies that do not depend on the eddy type. Eddies A1, C2 and C3 coincide with an enhancement of chlorophyll, whereas J98 shows a chlorophyll minimum. Eddy A1 was generated by Tenerife island 3 months before, and C2 was generated by La Palma island 2.5 months before. As eddy A1 was generated by Tenerife its enhancement of chlorophyll may not be attributed to entrainment by upwelling filaments, and therefore this increase is most likely related to eddy secondary circulation (eddy/wind interaction). Therefore, the Canary Eddy Corridor eddies PP not only affect locally but also all along the Corridor extension.

To place in context the influence of the Canary Eddy Corridor on the PP of the region we first need to derive an average value of PP per eddy (Table 3). Barton et al. (1998) estimated a PP of 7.3 molN m^2 yr^{-1} (=1.6 g C m^{-2} d^{-1}) for a Gran Canaria cyclone at its early stage of formation with an estimated vertical velocity of w=7.5 m d^{-1}. Benitez-Nelson et al. (2007), reported a similar value of PP=1.5 g C m^{-2} d^{-1}, also for a cyclone at its early stage, generated by the island of Hawaii. Finally, McGillicuddy et al. (2007), estimate a PP in a mid-ocean anticyclone of

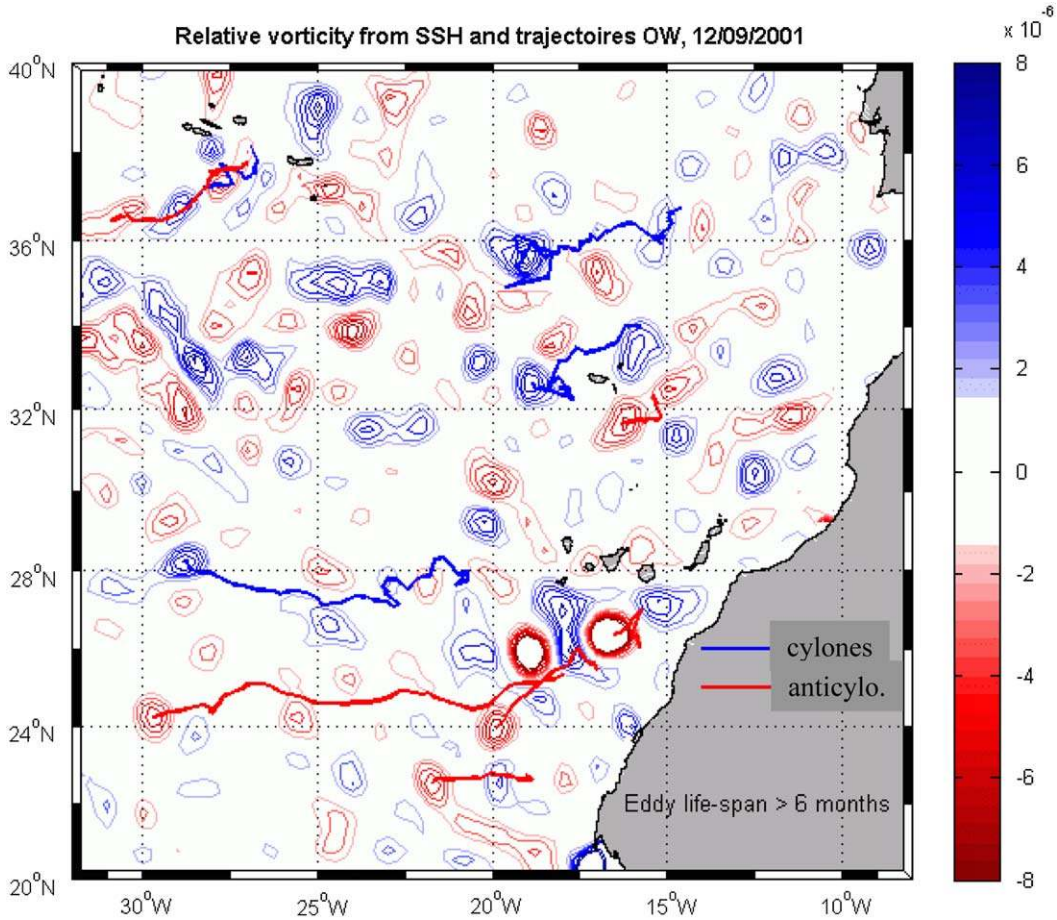

Fig. 11. Vorticity distribution in the study domain corresponding to the date in Fig. 2c. Tracks are trajectories of eddies with life-spans greater than 6 months.

PP=0.6 g C m^{-2} d^{-1} with an associated vertical velocity of w=0.4 m d^{-1}. Note that cyclonic eddies have PP 3 times higher than the mid-ocean anticyclone, coinciding with higher vertical velocities. Note also from Fig. 4 that chlorophyll concentration for cyclones, at their early stage of formation, are higher. Therefore, an average estimate of PP in the Canary Eddy Corridor (formed by cyclonic and anticyclonic eddies) could be PP=1 g C m^{-2} d^{-1} per eddy. This value is one order of magnitude higher than the PP measured in the far-field waters (not affected by the eddy field) of the Canary region (Barton et al., 1998). Anticyclones of the Corridor are as intense, or more intense, than the anticyclone A4 described by McGillicuddy et al. (2007), where a plankton bloom was observed (compare Fig. 1 of McGillicuddy et al. (2007) with anomalies derived from Fig. 3c). On the other hand, mean Trade Wind intensity in our region is about 8 m s^{-1} (Barton et al., 1998), larger than mean wind intensity observed by McGillicuddy et al. (2007). Therefore, the difference between air and water velocities in our region, which could drive plankton blooms on anticyclones, can be as intense or more intense than those observed by McGillicuddy et al. (2007).

In order to estimate the total primary production by the Canary Eddy Corridor, we have multiplied the average PP per eddy (1 g C m^{-2} d^{-1}) by the area of the 17 annually generated long-lived eddies (Table 3), giving us a total value: total Canary corridor production (PET)=13.3 $\times$ 10^{10} g C d^{-1}. As the Corridor eddies spend more than 1 year crossing the entire domain we can expect a mean of 17 eddies simultaneously occupying the Corridor. As an example, in Fig. 11 we show the vorticity distribution along our whole domain for the same day as Fig. 2c, where more than 17 eddies occupy the Canary Eddy Corridor region.

Pelegrí et al. (2005a, b) reviewed the reported values of PP on the northwest African Upwelling System (NAUS) estimating a mean value of 2.4 $\pm$ 1.5 g C m^{-2} d^{-1}, about two times higher than our estimate of the Canary Eddy Corridor (Table 3). We can estimate the total primary production of the NAUS by multiplying its mean value by the NAUS area between the latitude range of the Canary Eddy Corridor (22°N–29°N), giving us a value of PUT=10.5 $\times$ 10^{10} g C d^{-1} (Table 3). The value coincides with total primary production by the Canary Eddy Corridor (see above and Table 3). This indicates that the Canary Eddy Corridor is as productive as the NAUS, suggesting that it may have a significant impact on biogeochemical fluxes in the northeastern subtropical Atlantic. As seen in the Supplementary Movie, eddy pulsations are very frequent, suggesting intermittence in the secondary circulation and, hence, quite frequent events of eddy fertilisation due to upward Ekman pumping velocities that are probably related to eddy/wind interactions (Martins and Richards, 2001; McGillicuddy et al., 2007).

Our results pose the question of whether the eastern North Atlantic subtropical gyre can be considered as an oligotrophic system. Nevertheless, these estimates should be taken as a first approach and, as they depend critically on the estimated primary production per eddy, effort should be made to improve these estimates.

Acknowledgements

This work was supported by the Spanish government through projects RODA (CTM2004-06842) and CANOA (CTM2005-00444/MAR), and by the US National Science Foundation project "Vorticity generation and eddy evolution in island wakes" (OCE 06-23011) and by NASA project "NNX08AI84G". The altimeter products were produced by Ssalto/Duacs and distributed by Aviso, with support from Cnes. A. Rubio was supported by a French CNRS postdoctoral fellowship. Many thanks to all three anonymous reviewers for their useful comments and suggestions.

Appendix A. Supplementary material

Supplementary data associated with this article can be found in the online version at doi:10.1016/j.dsr.2009.08.008.

References

Alonso-González, I.J., Arístegui, J., Vilas, J.C., Hernández-Guerra, A., 2009. Lateral POC transport and consumption in surface and deep waters of the Canary Current region: a box model study. Global Geochemical Fluxes, in press.

Arístegui, J., Sangrà, P., Hernández-León, S., Cantón, M., Hernández_-Guerra, A., Kerling, J.L., 1994. Island-induced eddies in the Canary Islands. Deep-Sea Research I 41, 1509–1525.

Arístegui, J., Tett, P., Hernández-Guerra, A., Basterretxea, G., Montero, M.F., Wild, K., Sangrà, P., Hernández-León, S., Cantón, M., García-Braun, J.A., Pacheco, M., Barton, E.D., 1997. The influence of island-generated eddies on chlorophyll distribution: a study of mesoscale variation around Gran Canaria. Deep-Sea Research I 44, 71–96.

Barton, E.D., Arístegui, J., Tett, P., Cantón, M., García-Braun, J., Hernández-León, S., Nykjaer, L., Almeida, C., Almunia, J., Ballesteros, S., Basterretxea, G., Escánez, J., García-Weill, L., Hernández-Guerra, A., López-Laatzeng, F., Molina, R., Montero, M.F., Navarro-Pérez, E., Rodríguez, J.M., van Lenning, K., Vélez, H., Wild, K., 1998. The transition zone of the Canary Current upwelling region. Progress in Oceanography 41, 455–504.

Benitez-Nelson, C.R., Bidigare, R.R., Dickey, T.D., Landry, M.R., Leonard, C.L., Brown, S.L., Nencioli, F., Rii, Y.M., Maiti, K., Becker, J.W., Bibby, T.S., Black, W., Cai, W.J., Carlson, C.A., Chen, F., Kuwahara, W.S., Mahaffey, C., McAndrew, P.M., Quay, P.D., Rappé, M.S., Selph, K.E., Simmons, M.P., Yang, E.J., 2007. Mesoscale eddies drive increased silica export in the Subtropical Pacific Ocean. Science 316, 1017–1021.

Calil, P.H.R., Kelvin, J., Richards, K.J., Jia, Y., Bidigare, R.R., 2008. Eddy activity in the lee of the Hawaiian Islands. Deep-Sea Research II 55, 1179–1194.

Carrère, L., Lyard, F., 2003. Modeling the barotropic response of the global ocean to atmospheric wind and pressure forcing—comparisons with observations. Geophysical Research Letters 30, L1275.

Chelton, D.B., Schlax, M.G., Samelson, R.M., Szoeke, R.A., 2007. Global observations of large oceanic eddies. Geophysical Research Letters 34, L15606.

Cushman-Roisin, B., Chassignet, E.P., Tang, B., 1990. Westward motion of mesoscale vortices. Journal of Physical Oceanography 20, 758–768.

Danabasoglu, G., Ferrari, R., McWilliams, J.C., 2008. Sensitivity of an ocean general circulation model to a parameterization of near surface eddy fluxes. Journal of Climate 21, 1192–1208.

Doglioli, A.M., Blanke, B., Speich, S., Lapeyre, G., 2007. Tracking coherent structures in a regional ocean model with wavelet analysis: application to Cape Basin eddies. Journal of Geophysical Research 112, C05043.

Ducet, N., Le Traon, P.Y., Reverdin, G., 2000. Global high resolution mapping of ocean circulation from the combination of TOPEX/POSEIDON and ERS-1/2. Journal of Geophysical Research 105, 19477–19498.

Eaton, B.E., 1987. Analysis of laminar vortex shedding behind a circular cylinder by computer-aided flow visualisation. Journal of Fluid Mechanics 180, 117–145.

Gabric, A.J., García, L., Van Camp, L., Nykjaer, L., Eifler, W., Schrimpf, W., 1993. Offshore export of shelf production in the Cap Blanc giant filament as derived from CZCS imagery. Journal of Geophysical Research 98, 4697–4712.

Graves, L.P., McWilliams, J.C., Montgomery, M.T., 2006. Vortex evolution due to straining: a mechanism for dominance of strong, interior anticyclones. Geophysical and Astrophysical Fluid Dynamics 100, 151–183.

Hernández-Guerra, A., Fraile-Nuez, E., López-Laatzen, F., Martínez, A., Parrilla, G., Vélez-Belchí, P., 2005. Canary Current and North Equatorial Current from an inverse box model. Journal of Geophysical Research 110, C12019.

Isern-Fontanet, J., Garcia-Ladona, E., Font, J., 2006. Vortices of the Mediterranean Sea: an altimetric perspective. Journal of Physical Oceanography 36, 87–103.

Jiménez, B., Sangrà, P., Mason, E., 2008. A numerical study of the relative importance of wind and topographic forcing on oceanic eddies shedding by deep water islands. Ocean Modelling 22, 146–157.

Jochum, M., Danabasoglu, G., Holland, M., Kwon, Y.O., Large, W.G., 2008. Ocean viscosity and climate. Journal of Geophysical Research 113, C06017.

Le Traon, P.Y., Ogor, F., 1998. ERS-1/2 orbit improvement using TOPEX/POSEIDON: the 2 cm challenge. Journal of Geophysical Research 103, 8045–8057.

Lévy, M., 2008. The modulation of biological production by mesoscale turbulence. Lecture Notes in Physics 744, 219–261.

Martin, A.P., Richards, K.J., 2001. Mechanisms for vertical nutrient transport within North Atlantic mesoscale eddy. Deep-Sea Research II 48, 757–773.

McGillicuddy, D.J., Anderson, L.A., Bates, N.R., Bibby, T., Buesseler, K.O., Carlson, C.A., Davis, C.S., Ewart, C., Falkowski, P.G., Goldthwait, S.A., Hansell, D.A., Jenkins, W.J., Johnson, R., Kosnyrev, V.K., Ledwell, J.R., Li, Q.P., Siegel, D.A., Steinberg, D.K., 2007. Eddy/Wind interactions stimulate extraordinary Mid-Ocean plankton Bloom. Science 316, 1021–1026.

Minobe, S., Kuwano-Yoshida, A., Komori, N., Xie, S.P., Small, R.J., 2008. Influence of the Gulf Stream on the troposphere. Nature 452, 206–209.

Navarro-Pérez, E., Barton, E.D., 1997. The physical structure of an upwelling filament of the North-West African Coast during August 99. South African Journal of Marine Science 19, 61–73.

Navarro-Pérez, T., Barton, E.D., 2001. Seasonal and interannual variability of the Canary Current. Scientia Marina 65 (Suppl. 1), 205–213.

Pacheco, M., Hernández-Guerra, A., 1999. Seasonal variability of recurrent phytoplankton pigment patterns in the Canary Islands area. International Journal of Remote Sensing 20, 1408–1495.

Pascual, A., Faugere, Y., Larnicol, G., Le Traon, P.Y., Rio, M.H., 2006. Improved description of the ocean mesoscale variability by combining four satellite altimeters. Geophysical Research Letters 33, L02611.

Pascual, A., Pujol, M.I., Larnicol, G., Le Traon, Y., 2007. Mesoscale mapping capabilities of multisatellite altimeter missions: first results with real data in the Mediterranean Sea. Journal of Marine Systems 65, 190–211.

Pelegrí, J.L., Arístegui, J., Cana, L., González, M., Hernández-Guerra, A., Hernández-León, S., Marrero-Díaz, A., Montero, M.F., Sangrà, P., Santana-Casiano, M., 2005a. Coupling between the open ocean and the coastal upwelling region off Northwest Africa: water recirculation and offshore pumping of organic matter. Journal of Marine Systems 54, 3–37.

Pelegrí, J.L., Marrero-Díaz, A., Ratsimandresey, A., Antoranz, A., Cisneros-Aguirre, J., Gordo, C., Grisolía, D., Hernández-Guerra, A., Láiz, I., Martínez, A., Parrilla, G., Pérez-Rodríguez, P., Rodríguez-Santana, A., Sangrà, P., 2005b. Hydrographic cruises off northwest Africa: the Canary Current and the Cape Ghir region. Journal of Marine Systems 54, 39–63.

Pelegrí, J.L., Marrero-Díaz, A., Ratsimandresey, A.W., 2006. Nutrient irrigation of the North Atlantic. Progress in Oceanography 70, 366–406.

Piedeleu, M., Sangrà, P., Sánchez-Vidal, A., Fabrés, J., Gordo, C., Calafat, A., 2009. An observational study of oceanic eddy generation mechanisms by tall deep-water islands (Gran Canaria). Geophysical Research Letters 36, L14605, doi:10.1029/2008GL037010.

Pingree, R.D., 1996. A shallow subtropical subduncting westward propagating eddy (Swesty). Philosphical Transactions of the Royal Society of London 354, 979–1026.

Pingree, R.D., Garcia-Soto, C., Sinha, B., 1999. Position and structure of the Subropical/Azores Front region from conbined Lagragian and remote sensing (IR/altimeter/Seawifs) measurements. Journal of the Marine Biological Association of the United Kingdom 79, 769–792.

Pingree, R.D., Garcia-Soto, C., 2004. Annual westward propagating anomalies near 26°N and eddy generation south of the Canary Islands: remote sensing (altimeter/SeaWIFS) and *in situ* measurements. Journal of the Marine Biological Association of the United Kingdom 84, 1105–1115.

Pingree, R.D., Sinha, B., 2001. Westward moving waves or eddies (*Storms*) on the Subropical/Azores Front near 32.5°N? Interpretation of the Eulerians currents and temperture records at morrings 155 (35.5°W) and 156 (34.4°W). Journal of Marine Systems 29, 239–276.

Rio, M.-H., Hernandez, F., 2004. A mean dynamic topography computed over the world ocean from altimetry, in-situ measurements and a geoid model. Journal of Geophysical Research 109, C12032, doi:10.1029/2003JC002226.

Sangrà, P., Pelegrí, J.L., Hernández-Guerra, A., Arregui, I., Martín, J.M., Marrero-Díaz, A., Martínez, A.W., Ratsimandresey, A., Rodríguez-Santana, A., 2005. Life history of an anticyclonic eddy. Journal of Geophysical Research 11, C03021.

Sangrà, P., Auladell, M., Marrero-Díaz, A., Pelegrí, J.L., Fraile-Nuez, E., Rodríguez-Santana, A., Martín, J.M., Mason, E., Hernández-Guerra, A., 2007. On the nature of oceanic eddies shed by the island of Gran Canaria. Deep-Sea Research I 54, 687–709.

Siegel, A., Weiss, J.B., 1997. A wavelet-packet census algorithm for calculating vortex statistics. Physics of Fluids 9, 1988–1999.

Small, R.J., deSzoeke, S., Xie, S.P., O'Neill, L., Seo, H., Song, Q., Cornillon, P., Spall, M., Minobe, S., 2008. Air–Sea interaction over oceanic fronts and eddies. Dynamics of Atmosphere and Oceans 45, 274–285.

Willett, S.C., Leben, R.R., Lavín, M.F., 2006. Eddies and tropical instability waves in the eastern tropical Pacific: a review. Progress in Oceanography 69, 218–238.